Journal of Sound and Vibration (2000) **231**(3), 727–737
doi:10.1006/jsvi.1999.2558, available online at http://www.idealibrary.com on IDEAL®

PREDICTION OF GROUND VIBRATION FROM TRAINS USING SEISMIC REFLECTIVITY METHODS FOR A POROUS SOIL

J. T. NELSON

Wilson, Ihrig & Associates, Inc., 5776 Broadway, Oakland, CA 94618, U.S.A.

(*Received in final form 23 September* 1999)

Biot's model of wave propagation in porous isotropic materials is explored for predicting ground vibration from rail vehicles on vertically heterogeneous isotropic saturated soil and rock using seismic reflectivity methods combined with a multi-degree-of-freedom model of a transit vehicle bogie. A sketch of the mathematical theory, canonical results for step loads on a porous half-space, spectral responses for simple layer profiles, and an example of a prediction for rail transit vehicles are presented. The model indicates that saturation of the soil introduces excess attenuation in the vibration response of the soil, and that both pitch and roll moments in addition to vertical forces caused by the vehicle bogie may be significant sources of vibration.

1. INTRODUCTION

This paper explores the application of Biot's theory [1, 2] to the prediction of ground vibration produced by rail transportation vehicles operating on layered porous soils. While simple analytical theories exist for predicting ground vibration from transit vehicles, the complex mathematical problem of vehicles operating on vertically heterogeneous layered soils is normally ignored, with some exceptions [3]. Early attempts at including porosity and fluid in models of vertically heterogeneous soils have primarily been in the area of seismic forward modelling. One of the first attempts at modelling wave propagation in vertically heterogeneous porous materials with smoothly varying porosity and moduli involved predicting solid and fluid responses to hydraulic fractures [4]. The formalism developed for hydraulic fracture modelling is applied here to model the response of layered soils to vertical loads and moments that might be caused by a transit vehicle. These forces and moments can be calculated by a multi-degree-of-freedom model of the vehicle bogie and track, using rail and wheel roughness profiles. The model can predict the effect of layering, porosity, depth to water table, and other characteristic parameters of soils.

0022-460X/00/130727 + 11 $35.00/0

2. MATHEMATICAL MODEL

The soil is modelled as a layered porous isotropic material supported on a homogeneous porous half-space. The atmosphere is assumed to cover the top of the layered soil structure. The equations of motion are well described in Biot's original papers concerning wave propagation in porous solids, and the formalism adopted by Biot in 1956 is used, where the porous matrix and fluid displacement are represented symmetrically.

Tortuosity and sinuosity parameters are incorporated in the density parameters, ρ_{ij}, introduced by Biot. The fluid viscosity is incorporated into the friction parameter, b, which accounts for dissipation due to relative flow between the fluid and porous matrix. The friction formulae introduced by Biot for slit pores are used here. At low frequencies, the friction is governed by Poiseuille flow, and at high frequencies, the friction is modified due to higher viscous shear stresses in the fluid. The transition between low and high frequencies is approximately 100 Hz for a pore size of 0·1 mm. For circular pores, the friction coefficient is similar to that given above if the pore size is changed by about 30%. Given the complex nature of pore geometries, the representation for slit-like pores is used here regardless of actual pore geometries that might be encountered.

The moduli of the saturated porous material, A, N, Q, and R, introduced by Biot, are assumed be functions of vertical position. Relations between these parameters were discussed by the author [4] and by Biot and Willis [5]. The problem concerning the stress–strain response is reduced to providing the shear and bulk moduli for the porous structure and a bulk modulus for the fluid, together with a porosity. In the present case, the elastic moduli for the porous structure in a "drained" condition, the bulk modulus for the fluid, and the porosity are specified, and the remaining parameters, A, Q, R, and density parameters are inferred. The specified parameters might be realized from actual laboratory or field tests of soils.

The solutions to the equation of motion for the matrix displacement and partial tractions acting at horizontal planes are represented in cylindrical co-ordinates, r, θ, and z, as

$$\hat{\mathbf{u}}(r, \theta, z, \omega) = \frac{1}{4\pi} \sum_{m=-\infty}^{m=+\infty} \int_0^\infty [l_1^m(k, z, \omega)\mathbf{T}_k^m(r, \theta) + r_1^m(k, z, \omega)\mathbf{S}_k^m(r, \theta) + r_2^m(k, z, \omega)\mathbf{R}_k^m(r, \theta)]\, k\, \mathrm{d}k$$

$$\hat{\mathbf{T}}(r, \theta, z, \omega) = \frac{1}{4\pi} \sum_{m=-\infty}^{m=+\infty} \int_0^\infty [l_2^m(k, z, \omega)\mathbf{T}_k^m(r, \theta) + r_3^m(k, z, \omega)\mathbf{S}_k^m(r, \theta) + r_4^m(k, z, \omega)\mathbf{R}_k^m(r, \theta)]\, k\, \mathrm{d}k$$

These expressions are identical in form with those employed by Aki and Richards for vertically heterogeneous elastic regions [6]. The variables k, and m, are the radial wavenumber and azimuthal mode number, respectively. The coefficients l_1, l_2, r_1, r_2, r_3 and r_4 are displacement-stress vector components which separate

into shear-horizontal (SH) and dilatational radial and vertical (PSV) solutions. The components l_1 and l_2 are the SH components, and r_1, r_2, r_3 and r_4 are the PSV components. Similar representations are used for the vertical components of fluid displacement and partial traction. Fluid shear is not included in the model, because the radial and transverse components of fluid displacement are not included in boundary conditions between layers, and the fluid partial traction acting on an element of area in the horizontal plane is necessarily oriented normal to the plane. Thus, only the vertical components of fluid displacement and traction are needed. The fluid displacement in the vertical direction is represented as

$$\hat{U}\hat{z}(r, q, z, \omega) = \frac{1}{4\pi} \sum_{m=-\infty}^{m=n+\infty} \int_0^\infty s_1^m(k, z, \omega)\mathbf{R}_k^m(r, \theta)k \, \mathrm{d}k$$

and the fluid partial traction (normal to the horizontal plane) is

$$\hat{S}\hat{z}(r, \theta, z, \omega) = \frac{1}{4\pi} \sum_{m=-\infty}^{m=+\infty} \int_0^\infty s_2^m(k, z, \omega)\mathbf{R}_k^m(r, \theta)k \, \mathrm{d}k.$$

The displacement–stress components s_1 and s_2 are coupled with the PSV displacement–stress components, r_1, r_2, r_3, and r_4, for the porous structure, and are thus part of the PSV solution. The cylindrical vector harmonics employed above are

$$\mathbf{T}_k^m(r, \theta) = \hat{r}\frac{1}{kr}\frac{\partial Y_k^m}{\partial \theta}(r, \theta) - \hat{\theta}\frac{1}{k}\frac{\partial Y_k^m}{\partial r}(r, \theta),$$

$$\mathbf{S}_k^m(r, \theta) = \hat{r}\frac{1}{k}\frac{\partial Y_k^m}{\partial r}(r, \theta) + \hat{\theta}\frac{1}{kr}\frac{\partial Y_k^m}{\partial \theta}(r, \theta),$$

$$\mathbf{R}_k^m(r, \theta) = -Y_k^m(r, \theta)\hat{z}, \quad Y_k^m(r, \theta) = J_m(kr)\mathrm{e}^{\mathrm{i}m\theta}.$$

$\mathbf{T}_k^m$ is associated with the shear horizontal motion (SH), and $\mathbf{S}_k^m$ and $\mathbf{R}_k^m$ are associated with the PSV response.

The time-transformed loads are similarly expanded in cylinder harmonics. For body forces applied to the porous matrix:

$$\mathbf{f}(r, \theta, z, \omega) = -\frac{1}{4\pi} \sum_{m=-\infty}^{m=+\infty} \int_0^\infty [f_T^m(k, z, \omega)\mathbf{T}_k^m(r, \theta) + f_S^m(k, z, \omega)\mathbf{S}_k^m(r, \theta) + f_R^m(k, z, \omega)\mathbf{R}_k^m(r, \theta)]k \, \mathrm{d}k.$$

The fluid loads are expressed as

$$\mathbf{F}(r, \theta, z, \omega) = -\frac{1}{4\pi} \sum_{m=-\infty}^{m=+\infty} \int_0^\infty [F_T^m(k, z, \omega)\mathbf{T}_k^m(r, \theta) + F_S^m(k, z, \omega)\mathbf{S}_k^m(r, \theta) + F_R^m(k, z, \omega)\mathbf{R}_k^m(r, \theta)]k \, \mathrm{d}k.$$

Solutions for the displacement–stress components within each heterogeneous layer are obtained for each frequency and radial wavenumber, k, by solving a set of ordinary differential equations in z [4]. These are used to construct propagators that represent fundamental solutions for each layer.

For the homogeneous porous half-space below the layered region, the solution is expressed with two scalar and two vector potentials, the solutions of which are used to provide boundary conditions at the bottom of the layered region. An additional scalar function is needed beyond the usual scalar potential for an elastic or viscoelastic region to represent the fluid displacement field. The vector potentials for rotational displacements of the fluid are proportional to the vector potentials for the structural displacements, and are thus redundant. The boundary conditions at the supporting half-space are satisfied by setting the coefficients of the upward propagating waves to zero, as there are no sources at positive infinity.

A fluid layer is included above the porous region as a matter of completeness. While it is not necessary, it admits the possibility of modelling acoustic sources. The upper layer is assumed to be air in the present work, for which a scalar potential representation is employed.

The boundary conditions at any horizontal plane or interface between layers include: continuity of normal, radial, and transverse displacements of the porous structure, continuity of the tangential partial tractions of the porous matrix, continuity of the sum of the normal partial tractions of the porous structure and fluid, continuity of fluid flux (fluid injection), and continuity of pore pressure. These conditions give eight boundary conditions at each horizontal surface. The solutions for the heterogeneous layers and the homogeneous half-spaces are substituted into a matrix equation representing the boundary conditions at each interface, and decomposed with a block-tridiagonal solver and LU decomposition. Solutions for various forces and displacement-gradients are obtained by back-substitution. The final solutions are obtained by numerical inversion of the Hankel transforms embodied in the above integral equations, using a Romberg integration scheme.

3. NUMERICAL SOLUTION

Figure 1 is a plot of the calculated vertical response of the surface of a half-space with uniform porous structure. Two cases are represented: one with air at standard pressure contained in the pores and the second with water. The porosity is assumed to be 50%, and pore size is assumed to be 0·2 mm. The shear and bulk stiffnesses for the drained condition were adjusted to provide an equivalent Poisson ratio for the drained matrix of 0·25. The distance from the source is 30 m.

The response for the dry condition is virtually identical with Pekeris' solution for the response of a uniform half-space to a vertical step load [7]. At the arrival time of the Rayleigh wave at about 0·23 s, there appears to be a slight over-shoot, which may be a result of the numerical inversion scheme, or might be due to a physical effect involving the structure and air cover. The P-wave arrival occurs at about 0·13 s, followed by a shear wave at about 0·2 s. With water introduced into the porous matrix, the P-wave arrival occurs much earlier, at about 0·03 s, though the maximum occurs at about 0·12 s. The shear wave is delayed until about 0·22 s, due to the added density. The Rayleigh arrival is heavily damped and much less well defined than for the case of air saturation alone. A permanent static displacement occurs because the step load remains applied for all time after 0 s. The two solutions

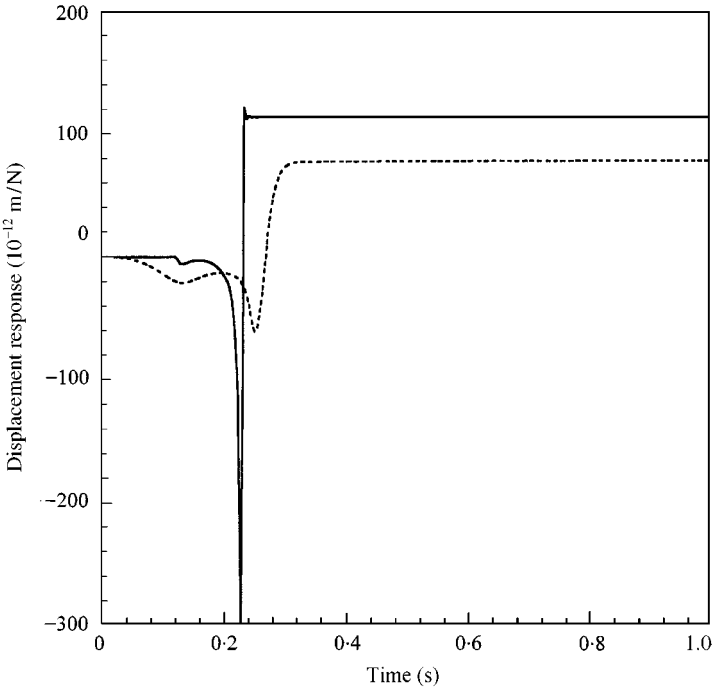

Figure 1. Vertical responses of uniform saturated and unsaturated porous half-spaces at 31 m from a 1 N vertical step point load applied at 0 s (Porosity = 0·5, Pore size = 0·2 mm): [— air saturated; ----- water saturated.]

are expected to agree asymptotically at large time, because the fluid is free to diffuse to the surface, and the reason for the lack of agreement has not been investigated. However, the discrepancy may be due simply to the method of calculating the static displacement over a finite time window, or it may be due to the manner of specifying the load. Further investigation is needed.

Figure 2 illustrates the evolution of the temporal response with distance from the source for the fluid saturated case. At 5 m, the response is quite strong, with a well-defined Rayleigh arrival. At larger distances, attenuation reduces both the amplitude and sharpness of the Rayleigh arrival. For the elastic case (not shown in Figure 2), there is no change of shape of the waveform, due to lack of a defining physical length. For the damped case, the pore size and attenuation rates provide a definition of length, so that the waveform changes shape with distance from the source.

Figure 3 illustrates the corresponding Fourier spectrum for the response to an impulse load. In this example, the high-frequency attenuation is very strong with increasing distance. At 80 Hz, the attenuation is 48 db at 30 m from the source relative to the response at 5 m. Numerical noise is evident in the solution for 31 m at about 120 Hz. Close to the source, the spectrum is flat.

The step responses for a uniform 6 m thick water saturated layer over a stiff half-space (rock) with small pore size is compared with the response to a saturated uniform half-space in Figure 4. The initial portions of each of the responses are

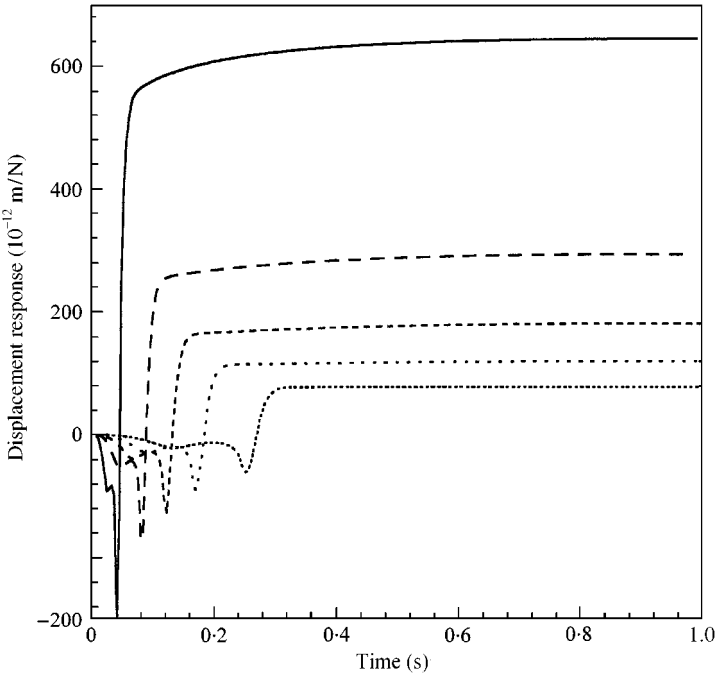

Figure 2. Vertical response of a uniform saturated porous half-space for a 1 N vertical step point load applied at 0 s (Porosity = 0·5, Pore size = 0·2 mm): —— 5 m; – – – 10 m; - - - 15 m; - - - - 21 m; · · · 31 m.

indistinguishable up to about 0·05 s, after which a reflection from the stiff layer tends to decrease the response relative to that of the uniform half-space. This would be the nature of a reflected P-wave from a layer of higher impedance. The shear-wave and Rayleigh wave arrivals occur at about the same time, 0·08 and 0·09 s. However, after 0·1 s, the response is greatly modified by the stiff layer, becoming a heavily damped sinusoid. Here, the layer produces a mode of vibration with a period of about 0·09 s.

Also shown in Figure 4 is the response of a 6 m thick heterogeneous layer with linearly increasing shear stiffness and bulk modulus with depth over the same stiff half-space. The porosity and pore size are assumed to be decreasing with increasing depth, as might be the case for a real soil. The response is very different from either of the other responses. Suprisingly, the calculated static deflection of the heterogeneous layer at the end of the 1 s time window is greater than that of the uniform layer.

Figures 5 illustrates the spectral responses at various distances for the fluid saturated heterogeneous layer introduced in Figure 4. The spectra are of the displacement Green's function, or responses to a delta function load, rather than the Heaviside step load. The spectrum nearest the source exhibits a flat characteristic, while at greater distances the spectra contain sharp dips or nodes. The maximum responses in the spectra occur at about 20–35 Hz at ranges of 15–31 m.

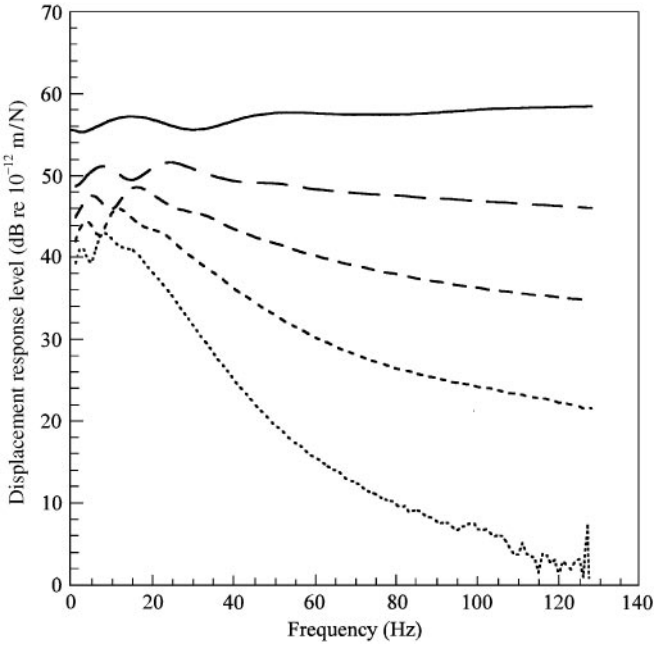

Figure 3. Vertical displacement response spectra (Green's function) for a saturated porous half-space excited by a 1 N s impulse (Porosity = 0·5, Pore size = 0·2 mm): —— 5 m; — — 10 m; – – –15 m; - - - - 21 m; ··· 31 m.

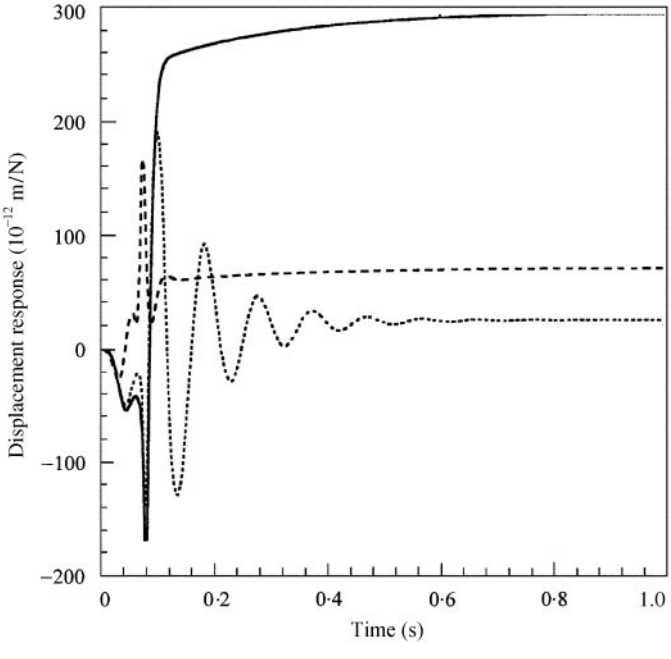

Figure 4. Vertical displacement responses of heterogeneous water saturated half-spaces at 10 m from a 1 N step load; —— Homogeneous half-space; ···homogeneous layer over stiff half-space at 6 m depth; - - - - heterogeneous layer over stiff-half-space.

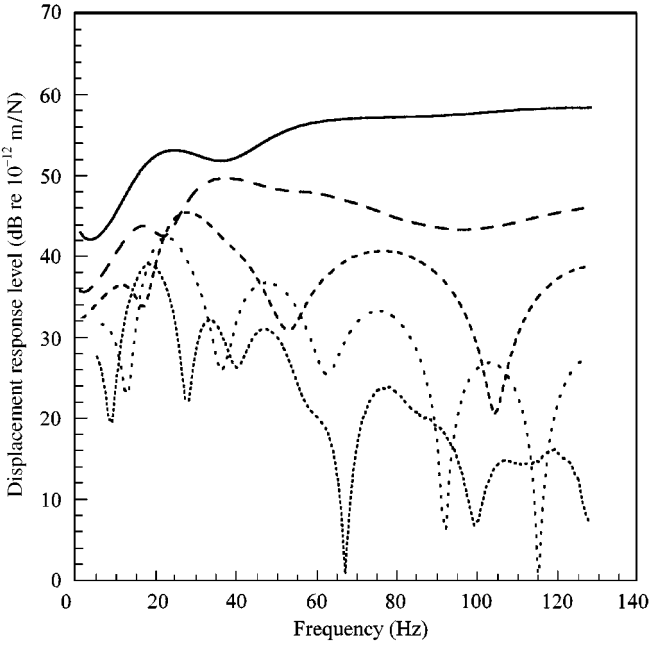

Figure 5. Vertical displacement response spectra (Green's function) of a 6 m thick heterogeneous saturated layer over a stiff rock-like half-space excited by a 1 N s impulse: —— 5 m; — — — 10 m; – – – – 15 m; - - - - 21 m; … 31 m.

4. PREDICTION OF TRAIN VIBRATION

The responses for the heterogeneous porous layer over a stiff layer are combined with the calculated forces and moments applied to the ground surface by a two-car articulated light-rail transit train and track with constant wheel and rail roughness amplitudes as a function of frequency. A multi-degree-of-freedom model of the motored and trailing trucks and of the track is used. The forces and moments are combined with the time derivatives of the Green's functions and those of the spatial gradients of the Green's functions for the heterogeneous layer discussed above, respectively. The spatial gradients were obtained by substituting inhomogeneous terms resulting from differentiating the Green's functions with respect to source co-ordinate in lieu of the force terms. The results are plotted in Figure 6 for the velocity response due to vertical forces caused by net vertical translation, moments transverse to the track caused by pitch, and moments parallel with the track caused by roll of the bogies. The energy sum of these contributions is also shown. Each wheel is assumed to have a roughness amplitude of 1 μm at all wavelengths, and the responses are summed incoherently for each wheel. Thus, a total of 24 sources are included. The curves are frequency response functions. Thus, if the sinusoidal roughness at the 50 Hz $\frac{1}{3}$ octave band is 1 μm, the corresponding $\frac{1}{3}$ octave band vibration velocity at 50 Hz would be about 26 dB re 1 μm/s, as given by the curve.

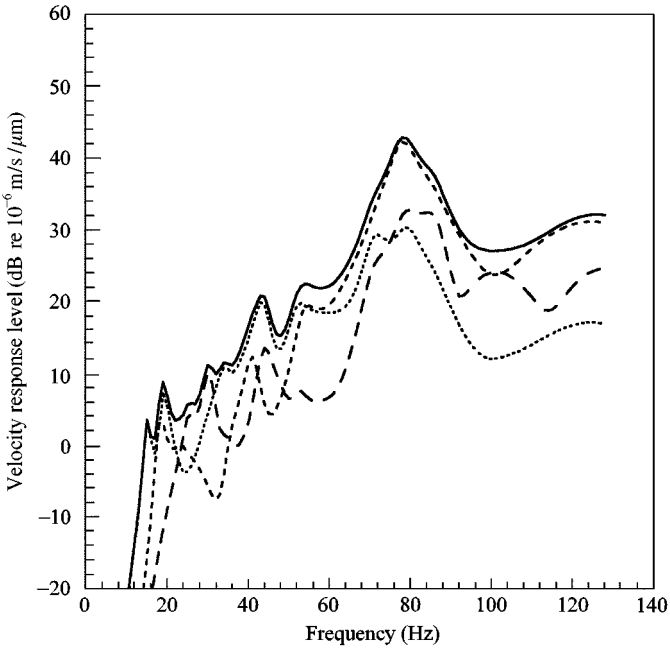

Figure 6. Vertical vibration velocity frequency response at 15 m from two articulated light-rail transit vehicles travelling at 40 kph with wheel sinusoidal roughness profiles of 1 μm: —— energy sum; – – – roll; - - - - pitch; ··· vertical force.

The spectra do not represent actual vibration velocity levels, because a realistic roughness spectrum is not included.

At low frequencies, the vertical forces dominate the response spectrum. However, at higher frequencies, the moments caused by pitch and roll become most significant. These results are surprising, because pitch and roll of the vehicle bogie are usually assumed to be less significant than the net vertical forces due to vertical translation of the bogie. This assumption is implicit in the experimental methods now employed for prediction of ground vibration at United States transit systems [8, 9].

Before concluding that pitch and roll moments are of similar or greater importance than vertical forces in calculating ground vibration, additional theoretical and experimental investigation is needed. For example, the roughnesses at each wheel are not incoherent. Each of 12 wheels on one side of the train rolls over the same roughness profile as the others. Secondly, each of the wheel roughnesses are periodic with wheel rotation, and corrugation at both rails may be coherent. The parametric excitation by the periodically spaced concrete ties is certainly correlated. Finally, the wavelength of Rayleigh waves in the soil are approaching the bogie dimensions at high frequencies, so that the assumption of a point moment acting on the surface is not realized, contrary to the assumption used here.

5. CONCLUSION

The model predictions should be compared with ground impulse responses at locations where responses have been measured and where soils reports are available. Rail and wheel roughness data at wavelengths important at ground vibration frequencies are needed, perhaps involving an extrapolation of Remington's estimates of roughness as a function of wavenumber [10]. Measurements of contact dynamic forces are needed to quantify vertical forces and pitch and roll moments of a bogie. The dissipation formula for the porous layer model should be developed further to include dissipation for partially saturated conditions. There exist energy dissipation formulae based on partial saturation which might be applicable [11]. A constant-Q loss factor for the porous matrix can be easily incorporated in the present model [4]. There are a number of factors that may frustrate application of the above methods to ground vibration prediction. These include lateral heterogeneity of the soil, folding, anisotropic material properties, etc.

ACKNOWLEDGMENTS

Much of the early work forming a basis for the present model was performed in the late 1980s at the Earth Science Division of the Lawrence Berkeley Laboratory of the University of California. Dr. Lane Johnson and Dr. Ernest Majer of the Earth Science Division provided support and valuable assistance in developing the theory. Professor Michael M. Carroll, now at Rice University, provided much inspiration and encouragement. Finally, the late M.A. Biot's lucid exposition of the theory of wave propagation in poro-elastic materials is invaluable.

REFERENCES

1. M. A. Biot 1956 *Journal of the Acoustical Society of America* **28**, 168–178. Theory of propagation of elastic waves in a fluid-saturated porous solid. I low frequency range.
2. M. A. Biot 1956 *Journal of the Acoustical Society of America* **28**, 179–191. Theory of propagation of elastic waves in a fluid-saturated porous solid. II higher-frequency range.
3. L. Auersch 1994 *Journal of Sound and Vibration* **173**, 233–264. Wave propagation in layered soils: theoretical solution in wavenumber domain and experimental results of hammer and railway traffic excitation.
4. J. T. Nelson 1988 *Doctoral Dissertation, Department of Mechanical Engineering, University of California at Berkeley*. Acoustic emission in a fluid saturated heterogeneous porous layer with application to hydraulic fracture.
5. M. A. Biot and D. G. Willis 1957 *Journal of Applied Mechanics* 594–601. The elastic coefficients of the theory of consolidation.
6. K. Aki and P. G. Richards 1980 *Quantitative Seismology, Theory and Methods, Vol. I and II*, 269. San Francisco: W. H. Freeman and Company.
7. C. L. Pekeris 1955 *Proceedings of the National Academy of Science U.S.A* **41**, 469–480. The seismic surface pulse.
8. C. Hanson, H. Saurenman, D. Towers, G. Anderson, Y. Kimura and W. Robert 1995 *Final Report, Harris Miller, & Hanson, Inc., for U.S. Department of Transportation, Federal Transit Administration. DOT-T-95-16*. Transit noise and vibration impact assessment.

9. J. T. Nelson and H. J. Saurenman 1987 *Environmental Issues*: *Noise*, *Rail Noise*, *and High-Speed Rail*, *Transportation Research Record* **1143**, 26–35. Prediction and control of groundborne noise and vibration from rapid transit systems.
10. P. J. Remington 1988 *Journal of Sound and Vibration* **120**, 203–226. Wheel/rail rolling noise: what do we know? What don't we know?, Where do we go from here?
11. G. M. Mavko and A. Nur 1978 *Geophysics* **44**, 161–178. Wave attenuation in partially saturated rocks.